Electrochimica Acta 109 (2013) 33–38

Contents lists available at ScienceDirect

Electrochimica Acta

journal homepage: www.elsevier.com/locate/electacta

Solid-state synthesis and electrochemical performance of $Li_4Ti_5O_{12}$/graphene composite for lithium-ion batteries

X. Guo [a], H.F. Xiang [a,*], T.P. Zhou [a], W.H. Li [b], X.W. Wang [c], J.X. Zhou [c], Y. Yu [b,**]

[a] Anhui Provincial Key Laboratory of Advanced Functional Materials and Devices, School of Materials Science and Engineering, Hefei University of Technology, Hefei, Anhui 230009, China
[b] CAS Key Laboratory of Materials for Energy Conversion, Department of Materials Science and Engineering, University of Science and Technology of China, Hefei, Anhui 230026, China
[c] Jiangsu Highstar Battery Manufacturing Co., Ltd., Nantong, Jiangsu 226200, China

ARTICLE INFO

Article history:
Received 20 May 2013
Received in revised form 7 July 2013
Accepted 7 July 2013
Available online 19 July 2013

Keywords:
Lithium titanate
Graphene
Solid-state reaction
Lithium-ion batteries

ABSTRACT

Homogeneous $Li_4Ti_5O_{12}$/graphene composite is prepared via an in-situ solid state reaction, after carbon pre-coating has been carried out. Its microstructure is compared with the materials prepared by a similar way, but without carbon coating. The results reveal that the carbon coating not only effectively confines aggregation and agglomeration of the $Li_4Ti_5O_{12}$ particles, but also enhances the combination between $Li_4Ti_5O_{12}$ particles and graphene sheets. The $Li_4Ti_5O_{12}$/graphene composite presents excellent rate capability and low-temperature performance. Even at 120 C, it still delivers a quite high capacity of about 136 mAh g^{-1}. When the charge–discharge tests are performed at −10 °C and −20 °C, its specific capacities are as high as 149 and 102 mAh g^{-1}, respectively. In addition, the full-cells using $LiNi_{1/3}Co_{1/3}Mn_{1/3}O_2$ as cathode material exhibit good rate capability.

1. Introduction

Lithium-ion batteries (LIBs) have been regarded as promising power sources for electric vehicles (EVs), owing to their advantages on energy density and lifetime. But the state-of-the-art LIBs based on the graphite anode can hardly meet the requirements of EVs on power density and safety characteristics [1]. Especially, limitation of lithium diffusion kinetics in the graphite crystals results in quite a long time to fully charge. Recently, novel candidates of graphite have attracted great interests, among which lithium titanate ($Li_4Ti_5O_{12}$, LTO) is the most promising for applications in the large-scale LIBs [2–8]. It exhibits excellent safety characteristics and long lifetime [7,8]. Moreover, nanosized $Li_4Ti_5O_{12}$ particles have short paths for lithium ion and electron transport and help to achieve fast charging for the LIBs [7]. However, the poor electronic conductivity of $Li_4Ti_5O_{12}$ restricts its rate performance [9,10]. Many approaches have been developed to solve this problem, including morphology tailoring and nanostructuring, ion doping, surface modification and mixing with some extraordinary conductive components [11–21]. Graphene, with excellent electronic conductivity, high surface area, outstanding thermal properties and mechanical strength, is considered as an ideal conductive additive to the nanostructured composites that used in LIBs and other electrochemical devices [22,23]. Hence the composites containing $Li_4Ti_5O_{12}$ and graphene have been widely investigated as high rate anode materials for lithium-ion batteries [24–29]. For example, Zhu et al. have fabricated graphene-embedded $Li_4Ti_5O_{12}$ nanofibers by electrospinning deposition [24]; Shen et al. and Tang et al. both prepared graphene–$Li_4Ti_5O_{12}$ hybrid nanostructures using a two-step hydrothermal reaction [25,26]; and we have prepared $Li_4Ti_5O_{12}$/graphene composite in a sol–gel method [27]. Ding et al. clarified the positive effects of graphene in $Li_4Ti_5O_{12}$/carbon composites as anode materials recently [29]. Although $Li_4Ti_5O_{12}$/graphene composites mentioned above exhibited good electrochemical performance, it still remains a great challenge to develop a facile and economical preparation route to achieve high performance $Li_4Ti_5O_{12}$/graphene composites. Solid state reaction is a commonly used method to prepare electrode materials in the battery industry. Nevertheless, to the best of our knowledge, there was no report that prepared homogeneous $Li_4Ti_5O_{12}$/graphene composites by an in situ solid state reaction.

Here in our investigation, inhomogeneity of $Li_4Ti_5O_{12}$/graphene composites results from facile stacking of graphene sheets and agglomeration of the $Li_4Ti_5O_{12}$ nanoparticles in a typical solid state reaction. By a carbon pre-coating process, we successfully overcomed this issue and prepared the homogeneous

* Corresponding author. Tel.: +86 551 62901360; fax: +86 551 6290136.
** Corresponding author. Tel.: +86 551 63607179; fax: +86 551 63602940.
E-mail addresses: hfxiang@hfut.edu.cn, xhfjj@scut.edu.cn (H.F. Xiang), yanyumse@ustc.edu.cn (Y. Yu).

0013-4686/$ – see front matter © 2013 Elsevier Ltd. All rights reserved.
http://dx.doi.org/10.1016/j.electacta.2013.07.058

$Li_4Ti_5O_{12}$/graphene composite in an in situ solid state reaction. The structure and morphology of the $Li_4Ti_5O_{12}$/graphene composites were investigated, and their cell performance was also evaluated, including rate capability and low-temperature performance.

2. Experimental

2.1. Materials preparation

The graphene sheets were prepared via a thermal exfoliation route, including graphite oxidation through modified Hummer method, followed by rapid thermal expansion of graphene oxide at 1050 °C in nitrogen atmosphere [30].

Anatase TiO_2 and glucose with a weight ratio of 4:1 were mixed in ethanol–water compounds (10:1 in volume) and stirred for 2 h, then drying for 10 h under air-circulating oven at 100 °C. The mixture was heated at 600 °C for 5 h under N_2 atmosphere to obtain the carbon coated TiO_2. The carbon content in the coated TiO_2 was about 6 wt.%.

Graphene, Li_2CO_3 and carbon-coated TiO_2 were dispersed in hexamethylene, and then mixed by balling milling, which was performed in a planetary ball mill (Nanjing) under atmosphere at rotational speed of 200 rpm for 4 h. The as-obtained slurry was dried and further calcined at 800 °C for 12 h in N_2 atmosphere to obtain the carbon-coated $Li_4Ti_5O_{12}$/graphene composites (denoted as C-LTO/graphene). In the composite, the total content of carbon including coated carbon and graphene sheets is about 10%. For comparison, pristine $Li_4Ti_5O_{12}$ (LTO) and $Li_4Ti_5O_{12}$/graphene composites without carbon coating (LTO/graphene) were prepared in a similar way.

2.2. Materials characterization

The crystal structure of the products was identified by X-ray diffraction (XRD) measurements (D/max 2500 V) using Cu Kα (λ = 1.5406 Å) radiation in the 2θ range of 10–70°. The morphology of the products was observed by scanning electron microscopy (SEM, JEOL JSM-6390LA) and transmission electron microscopy (TEM, JEM-2100F).

2.3. Electrochemical measurements

The electrochemical performance of the products was evaluated in coin-type cells. In order to make an electrode laminate, a uniform slurry containing 84 wt.% active material, 8 wt.% acetylene black and 8 wt.% polyvinylidene fluoride (PVDF) dispersed in N-methyl-2-pyrrolidinone (NMP) was cast onto an copper current collector. After vacuum drying at 70 °C, the laminate was punched into discs (Φ 14 mm) for assembling the cells. The mass loading in the electrode was controlled at about 5 mg cm^{-2}. In the half-cells, various LTO materials were used as working electrode and high-purity lithium metal as counter electrode. In the full-cells, the $LiNi_{1/3}Co_{1/3}Mn_{1/3}O_2$ positive electrode prepared in a similar way (just the current collector was replaced with aluminium foil) and the C-LTO/graphene negative electrode had the same mass loading, and the cell capacity was calculated on the mass of $LiNi_{1/3}Co_{1/3}Mn_{1/3}O_2$. The electrolyte was a solution of 1 M $LiPF_6$ in a mixture of ethylene carbonate (EC) and diethyl carbonate (DEC) (1:1, w/w). The separator is Celgard 2400 microporous polypropylene membrane. The cell performance of samples was evaluated on a multi-channel battery cycler (Neware BTS2300). Galvanostatic charge–discharge tests were performed under different current rates, where 1 C is corresponding to the current density of 150 mA g^{-1}. For the half-cells and the full-cells, the cut-off voltages were set as 2.5–1.0 V and 3.0–1.0 V, respectively. The temperature for the low-temperature performance measurements was controlled by a low-temperature chamber (Shanghai Yiheng Instruments Co., Ltd.). The AC impedance spectrum of the cells was measured by a CHI 604D electrochemical workstation (Shanghai Chenhua Instruments Co., Ltd.) in the frequency range from 10 mHz to 100 kHz with a potential perturbation at 5 mV.

3. Results and discussion

The crystal structures of $Li_4Ti_5O_{12}$ and its graphene composites are identified as shown in Fig. 1. The diffraction peaks of the pristine LTO, LTO/graphene composite and C-LTO/graphene composite are similar and conform to JCPDS card No.49-0207 in accordance with the spinel $Li_4Ti_5O_{12}$ phase with *Fd*3*m* space group. The narrow diffraction peaks indicate that $Li_4Ti_5O_{12}$ in the three samples are all highly crystalline. Similar as the XRD patterns of most $Li_4Ti_5O_{12}$/C composites [6,31,32], no any diffraction according to graphitic structure was detected, mainly due to the amorphous structure of coated carbon and graphene sheets. All the results indicate that the addition of graphene sheets and carbon-coating have no impact on the crystal structure and crystallinity of spinel $Li_4Ti_5O_{12}$ in the solid state reaction.

Fig. 2 shows SEM images of LTO, LTO/graphene, C-LTO/graphene and TEM image of C-LTO/graphene composite, respectively. As shown in Fig. 2a, the $Li_4Ti_5O_{12}$ primary particles are 200–800 nm in size and they are apt to aggregate together. The image of LTO/graphene (Fig. 2b) shows that the $Li_4Ti_5O_{12}$ particles are almost separated with graphene sheets. Moreover, particle size and aggregation degree of $Li_4Ti_5O_{12}$ in the LTO/graphene composite are similar to the pristine $Li_4Ti_5O_{12}$. Seemingly, it is difficult for bare LTO particles to stably anchor on the graphene sheets. Especially, aggregation of the $Li_4Ti_5O_{12}$ nanoparticles and further agglomeration result in inhomogeneity of $Li_4Ti_5O_{12}$/graphene composites and even phase separation. From the images of C-LTO/graphene composite (Fig. 2c and d), it can be seen that the $Li_4Ti_5O_{12}$ particles are quite uniformly dispersed among a three-dimensional network built by the graphene sheets, even though a few agglomerates are still inevitable in the high-temperature solid state reaction. The graphene network gives a conductive connection between the $Li_4Ti_5O_{12}$ particles. The size of most $Li_4Ti_5O_{12}$ particles is less than 100 nm (Fig. 2d). Furthermore, as revealed by the TEM image in Fig. 2d inset, the coated carbon layer has a thickness of less 10 nm. Basically, it can be easily concluded that the homogeneous

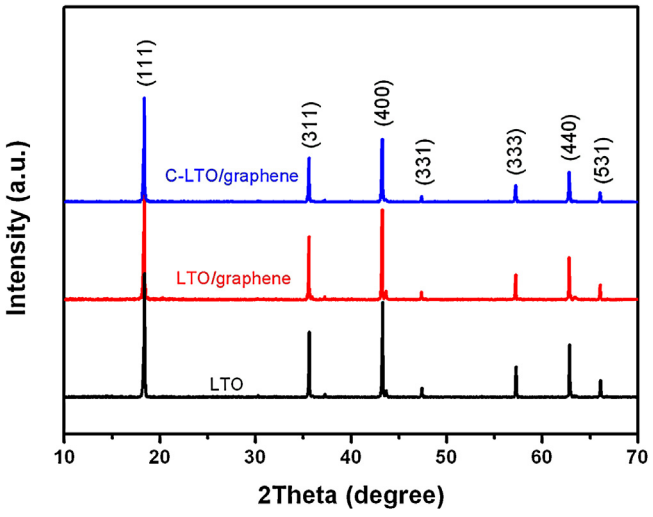

Fig. 1. XRD patterns of purified LTO, LTO/graphene composite and C-LTO/graphene composite.

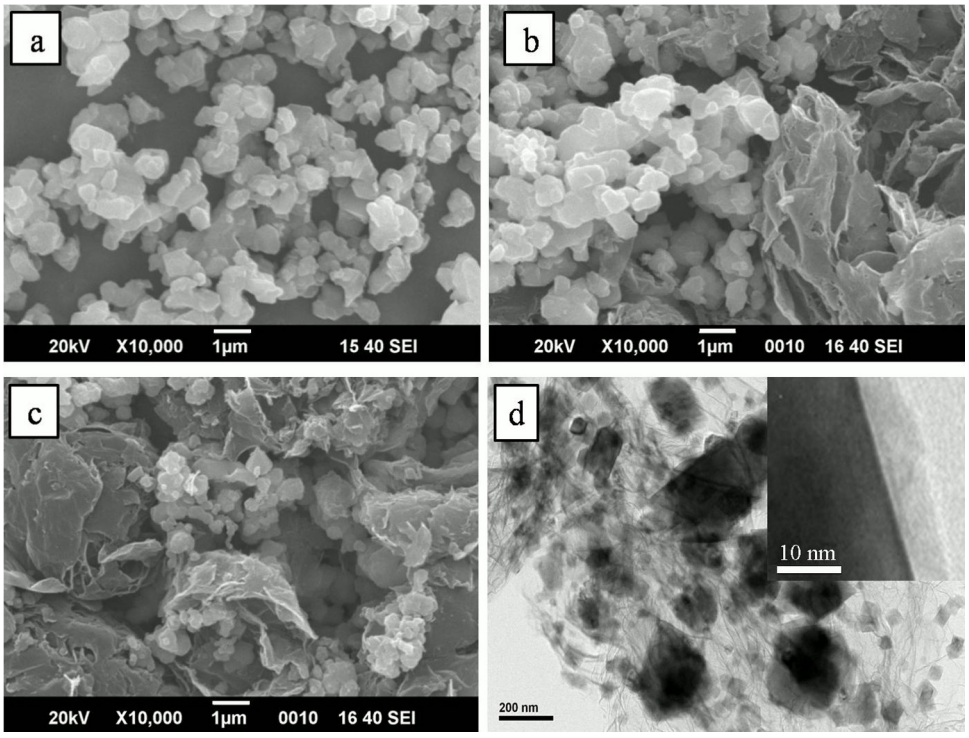

Fig. 2. SEM images of (a) LTO, (b) LTO/graphene, (c) C-LTO/graphene and TEM image (d) of C-LTO/graphene.

$Li_4Ti_5O_{12}$/graphene composite can be prepared in a solid state reaction with the help of carbon pre-coating.

The specific capacities of these samples were measured by charge–discharge test at constant current. Fig. 3 presents the first charge (lithium insertion) and discharge (lithium extraction) curves of these samples at 0.2 C (1 C = 150 mA g^{-1}) rate over the potential range of 1.0–2.5 V. It can be observed that the pristine LTO, LTO/graphene composite and C-LTO/graphene composite have similar charge and discharge plateaus, indicating that small quantity of graphene sheets do not affect the electrochemical reaction process of LTO. All the products display very flat charge–discharge plateaus at around 1.55 V (vs. Li/Li^+), demonstrating the characteristic of two-phase reaction based on the Ti^{4+}/Ti^{3+} redox couple. For the pristine LTO and LTO/graphene composite, the reversible capacities (discharge capacities) are 158 mAh g^{-1} and 163 mAh g^{-1}, respectively. However, the C-LTO/graphene composite delivers a high reversible capacity of 177 mAh g^{-1}, which is even higher than the theoretical capacity of $Li_4Ti_5O_{12}$ (175 mAh g^{-1}). The increased capacity can be attributed to lithium storage on the graphene sheets [30]. Herein, it can be easily found that carbon pre-coating obviously enhances lithium storage capability of the $Li_4Ti_5O_{12}$/graphene composite, in comparison of LTO/graphene and C-LTO/graphene.

Fig. 4 shows the reversible capacity vs. cycle number of the pristine LTO, LTO/graphene and C-LTO/graphene composites at different charge and discharge C-rates. Although the LTO/graphene composite presents higher specific capacity than LTO at high rates, the capacities of both LTO and LTO/graphene composite drop dramatically with increasing current rate and only show disappointing capacity of about 30–40 mAh g^{-1} at 10 C rate. As for the

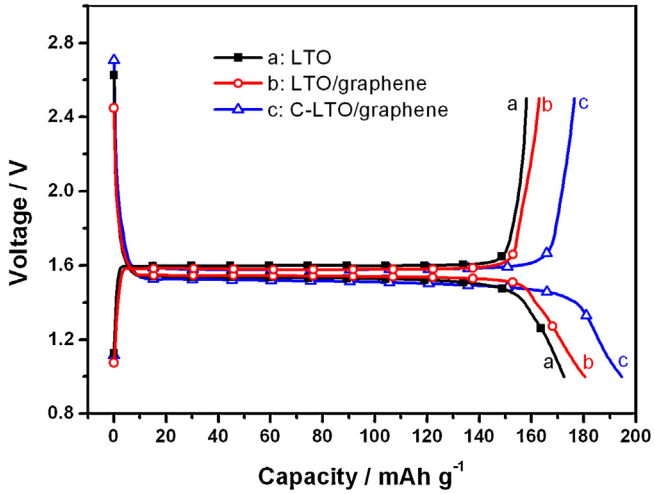

Fig. 3. Galvanostatic charge–discharge curves of LTO, LTO/graphene, C-LTO/graphene samples at 0.2 C charge–discharge rate.

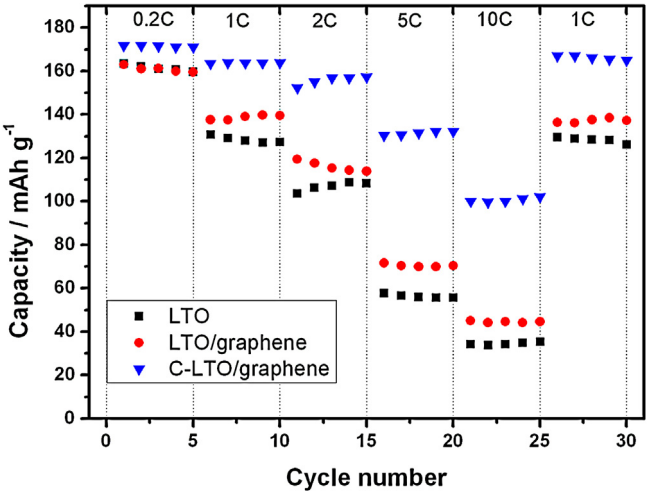

Fig. 4. Reversible capacity of LTO, LTO/graphene and C-LTO/graphene products at different charge–discharge rates.

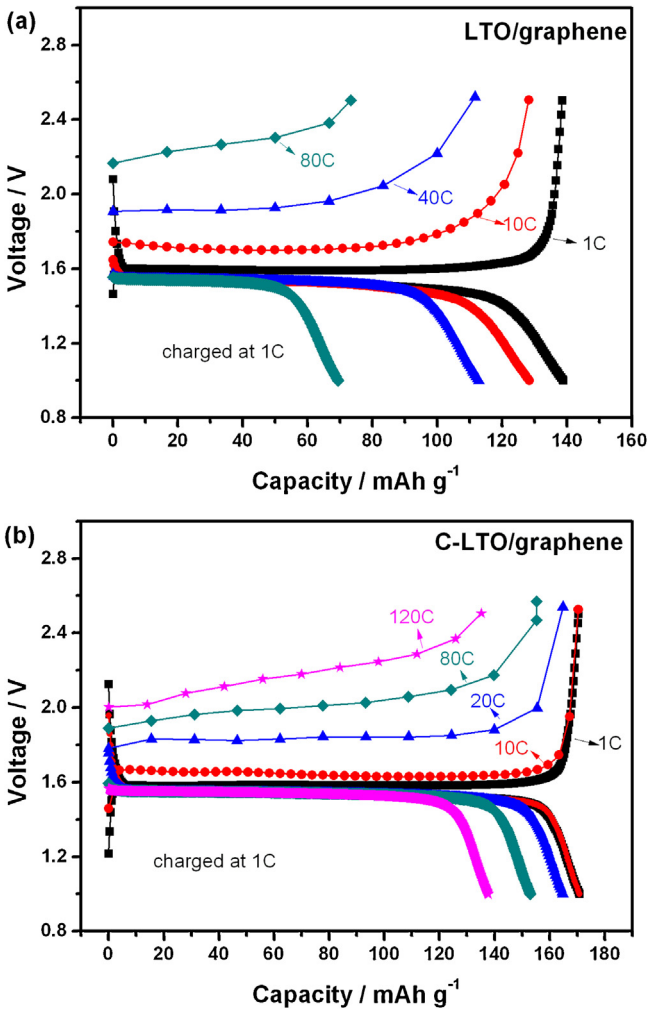

Fig. 5. Charge and discharge curves of (a) LTO/graphene and (b) C-LTO/graphene samples that discharge at 1 C and charged at different rates.

C-LTO/graphene composite, the capacities are superior to those of LTO and LTO/graphene composite at all charge/discharge rates. It should be noted that the specific capacity of the C-LTO/graphene composite is about 102 mAh g^{-1} at 10 C. Such a high capacity can be delivered in 4 min, after the batteries using the C-LTO/graphene composite anode has been charged for only 4 min. These results strongly suggest that the C-LTO/graphene composite is a promising fast-charging anode material. In addition, after the low current rate of 1 C is used again, the specific capacities of all the cells are restored, which suggests that $Li_4Ti_5O_{12}$ and its composites all exhibit good cyclic performance and excellent electrochemical stability.

For the LIBs applied in the EVs, currently available graphite anode cannot meet the power requirements of vehicles at start-up or speedup, where most lithium extraction from the anode materials should be executed in several to dozens of seconds. Hence, it is significant to evaluate the discharge capability (lithium extraction) of anode materials at high current rates. Before discharge at each rate, the cells were charged at 1 C. For the LTO/graphene composite (Fig. 5a), the discharge capacity is 139 mAh g^{-1}, and gradually reduced to 129, 112 and 74 mAh g^{-1} at rates of 10 C, 40 C and 80 C, respectively. Along with the discharge current rate increasing, the variations of discharge plateau potential are quite distinct. However, as shown in Fig. 5b, the C-LTO/graphene composite exhibits a very high reversible capacity of 155 mAh g^{-1} at 80 C, which is as twice as that of the LTO/graphene composite (70 mAh g^{-1} at 80 C).

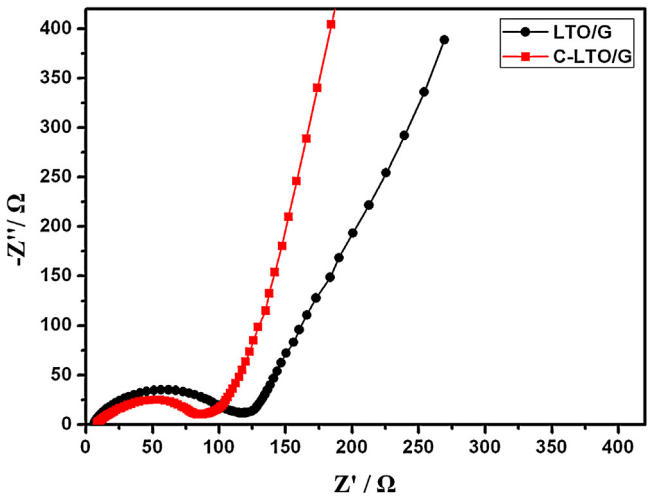

Fig. 6. AC impedance spectra of LTO/graphene and C-LTO/graphene at the state of full charged.

Even at 120 C, which corresponds to a discharge time of 28 s, the capacity is still as high as 136 mAh g^{-1}. Moreover, the discharge plateau potential of the C-LTO/graphene composite at 120 C is lower than that of the LTO/graphene composite at 80 C, which indicates

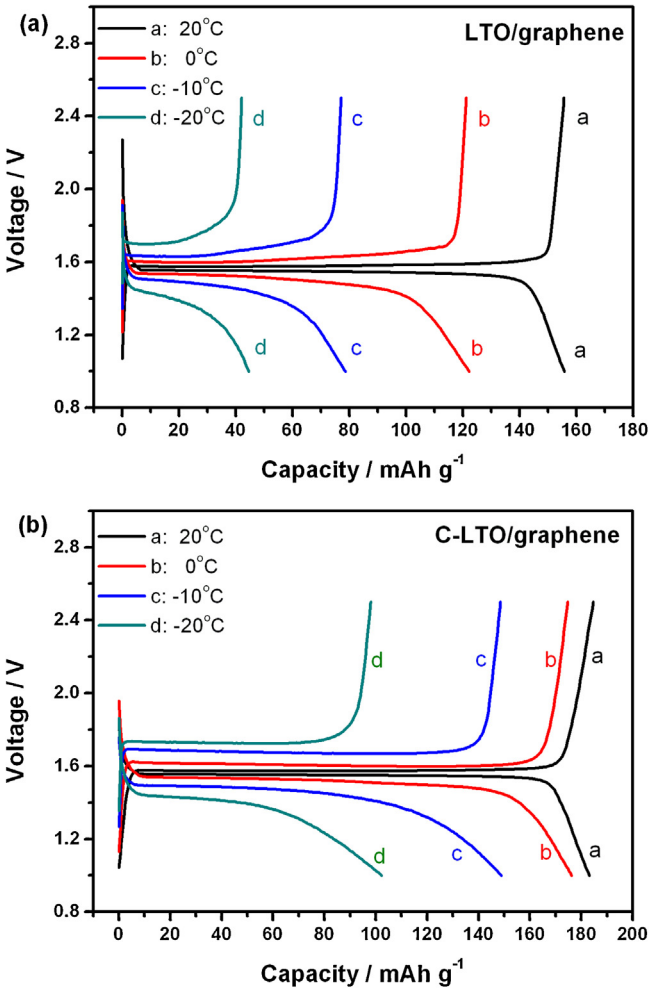

Fig. 7. Discharge and charge curves of (a) LTO/graphene and (b) C-LTO/graphene anode at 0.2 C rate at various temperatures.

that the C-LTO/graphene composite has lower polarization and better reaction kinetics.

Fig. 6 presents the AC impedance spectra of the cells using the LTO/graphene and C-LTO/graphene composites. The impedance curves show a semicircle in the high-to-medium frequency region and an inclined line in the low frequency region. The semicircle could be assigned to the charge transfer impedance and the inclined line could be considered as Warburg impedance. Here it is clear that the C-LTO/graphene composite has lower charge transfer impedance than the LTO/graphene composite, indicating the faster transfer rate of Li ions in the C-LTO/graphene composite because of its enhanced electronic conductivity.

For practical application as power sources of EVs, low-temperature performance of lithium-ion batteries should have attracted more attention. Here we have investigated the low-temperature performance of the LTO/graphene composite and the C-LTO/graphene composite. As shown in Fig. 7, the LTO/graphene composite exhibits reversible capacities of 155 mAh g^{-1} at 20 °C, 122 mAh g^{-1} at 0 °C, 78 mAh g^{-1} at −10 °C and only 45 mAh g^{-1} at −20 °C. However, the C-LTO/graphene composite delivers a capacity of about 183 mAh g^{-1} at 20 °C, 175 mAh g^{-1} at 0 °C, 149 mAh g^{-1} at −10 °C, and 102 mAh g^{-1} at −20 °C. From −10 °C to −20 °C, the capacity of C-LTO/graphene has a sharp drop mainly because of obviously reduced conductivity of the electrolyte [33]. It should be noted that the low-temperature performance of C-LTO/graphene composite could be improved further if the electrolyte is optimized. We are not aware of such good low-temperature performance for other anode materials reported in the literature.

To investigate the potential of the C-LTO–graphene anode material for industrial application, the full-cells using $LiNi_{1/3}Co_{1/3}Mn_{1/3}O_2$ as cathode material were assembled. As shown in Fig. 8, the full-cell delivers quite a high capacity of 116 mAh g^{-1} at 1 C, and retains 82% of this capacity at 8 C, which actually corresponds to a discharge time of 5 min. Therefore, the C-LTO/graphene anode material is of great potential for the application in high rate lithium-ion batteries.

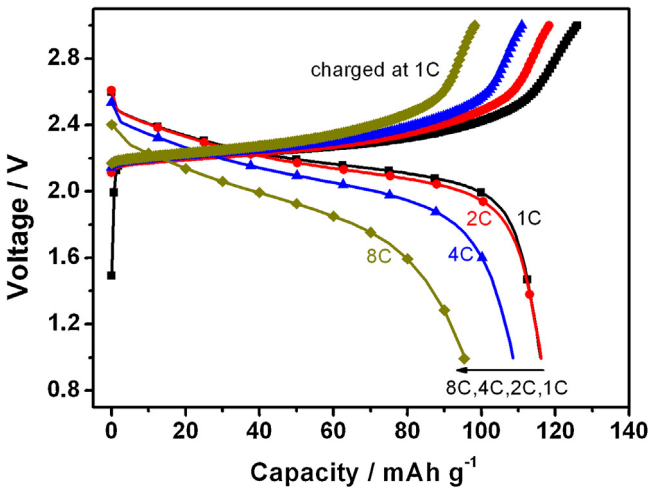

Fig. 8. Charge and discharge curves of the full-cell consisting of the C-LTO/graphene negative electrode and the $LiNi_{1/3}Co_{1/3}Mn_{1/3}O_2$ positive electrode at different discharge rates.

The superior electrochemical performance of C-LTO/graphene composites may be attributed to three aspects (as illustrated in Fig. 9). Firstly, carbon coating reduced the surface difference between $Li_4Ti_5O_{12}$ particles and graphene sheets, and so enhanced

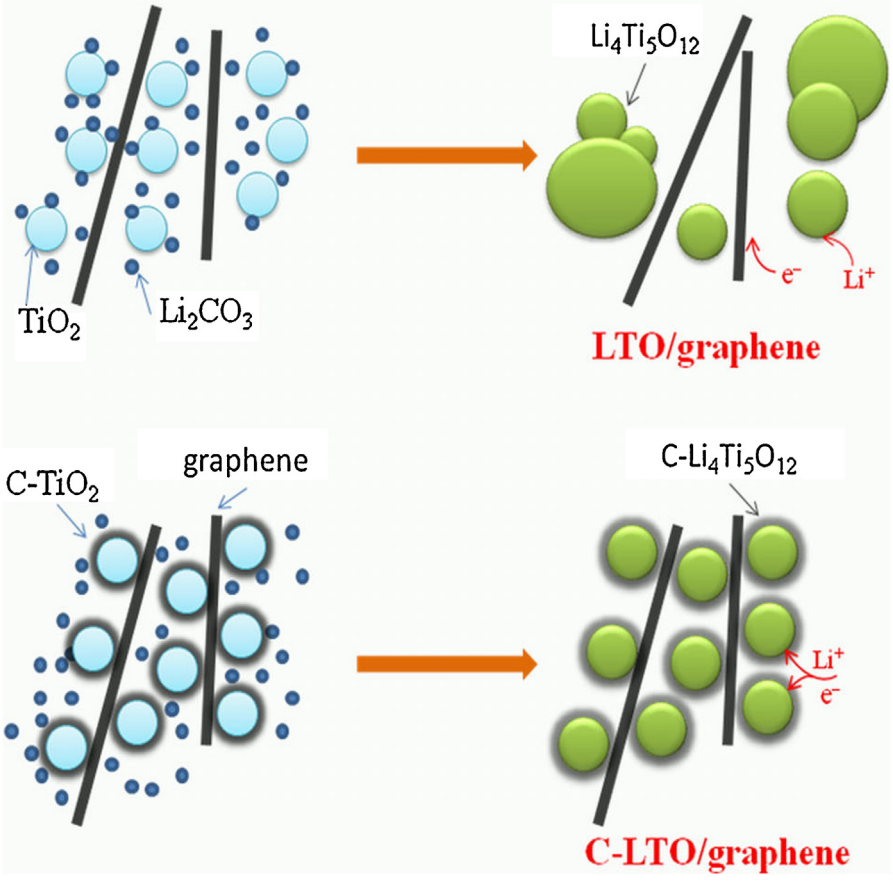

Fig. 9. Schematic illustration of the effects of carbon coating in LTO/graphene composites.

the interaction between $Li_4Ti_5O_{12}$ particles and graphene sheets directly. The carbon coated on the $Li_4Ti_5O_{12}$ particles acted as "binder" anchoring $Li_4Ti_5O_{12}$ particles on the graphene sheets firmly and help to obtain homogenous composites. Secondly, carbon pre-coating restrained the aggregation and agglomeration of $Li_4Ti_5O_{12}$ particles during solid-state sintering, which also contributed to the formation of stable and homogeneous LTO/grapheme composites. Moreover, the small particle size facilitated both electrons and lithium ions transport by reducing diffusion paths, and improved the electrochemical reaction kinetics by providing a larger electrode/electrolyte contact area. Thirdly, the uniform dispersion of the LTO particles on graphene sheets and their intimate interaction increased the electric conductivity of the LTO/graphene composites.

4. Conclusion

In summary, the homogeneous $Li_4Ti_5O_{12}$/graphene composites with superior lithium storage capability have been prepared by a solid state reaction. Carbon pre-coating is not only helpful to restrict aggregation and agglomeration of the $Li_4Ti_5O_{12}$ particles, but also effective to stick the $Li_4Ti_5O_{12}$ particles and graphene sheets together. The homogeneous and stable structures endow the $Li_4Ti_5O_{12}$/graphene composites with high-rate transportation for Li ions and electrons, and result in the good cell performance of the $Li_4Ti_5O_{12}$/graphene composites. Especially, their excellent rate capability and low temperature performance are of great importance for possible applications in EVs and HEVs. Here the facile solid state preparation for high-performance $Li_4Ti_5O_{12}$/graphene composites is quite attractive for large-scale industrialization.

Acknowledgements

This study was supported by National Science Foundation of China (Grant Nos. 21006033 and 21171015) and the Fundamental Research Funds for the Central Universities (2013HGCH0002).

References

[1] J.M. Tarascon, M. Armand, Issues and challenges facing rechargeable lithium batteries, Nature 414 (2001) 359.
[2] T. Ohzuku, A. Ueda, N. Yamamoto, Zero-strain insertion material of $Li[Li_{1/3}Ti_{5/3}]O_4$ for rechargeable lithium cells, Journal of the Electrochemical Society 142 (1995) 1431.
[3] K. Zaghib, M. Simoneau, M. Armand, M. Gauthier, Electrochemical study of $Li_4Ti_5O_{12}$ as negative electrode for Li-ion polymer rechargeable batteries, Journal of Power Sources 81–82 (1999) 300.
[4] K. Nakahara, R. Nakajima, T. Matsushima, H. Majima, Preparation of particulate $Li_4Ti_5O_{12}$ having excellent characteristics as an electrode active material for power storage cells, Journal of Power Sources 117 (2003) 131.
[5] Y. Wang, H. Liu, K. Wang, H. Eiji, Y. Wang, H. Zhou, Synthesis and electrochemical performance of nano-sized $Li_4Ti_5O_{12}$ with double surface modification of Ti(III) and carbon, Journal of Materials Chemistry 19 (2009) 6789.
[6] H.-G. Jung, S.-T. Myung, C.S. Yoon, S.-B. Son, K.H. Oh, K. Amine, B. Scrosati, Y.-K. Sun, Microscale spherical carbon-coated $Li_4Ti_5O_{12}$ as ultra high power anode material for lithium batteries, Energy and Environmental Science 4 (2011) 1345.
[7] L. Zhao, Y.S. Hu, H. Li, Z.X. Wang, L.Q. Chen, Porous $Li_4Ti_5O_{12}$ coated with N-doped carbon from ionic liquids for Li-ion batteries, Advanced Materials 23 (2011) 1385.
[8] G.N. Zhu, Y.G. Wang, Y.Y. Xia, Ti-based compounds as anode materials for Li-ion batteries, Energy and Environmental Science 5 (2012) 6652.
[9] L. Cheng, X.L. Li, H.J. Liu, H.M. Xiong, P.W. Zhang, Y.Y. Xia, Carbon-coated $Li_4Ti_5O_{12}$ as a high rate electrode material for Li-ion intercalation, Journal of the Electrochemical Society 154 (2007) A692.
[10] J.J. Huang, Z.Y. Jiang, The preparation and characterization of $Li_4Ti_5O_{12}$/carbon nano-tubes for lithium ion battery, Electrochimica Acta 53 (2008) 7756.
[11] B.B. Tian, H.F. Xiang, L. Zhang, Z. Li, H.H. Wang, Niobium doped lithium titanate as a high rate anode material for Li-ion batteries, Electrochimica Acta 55 (2010) 5453.
[12] K. Mukai, K. Ariyoshi, T. Ohzuku, Comparative study of $Li[CrTi]O_4$, $Li[Li_{1/3}Ti_{5/3}]O_4$ and $Li_{1/2}Fe_{1/2}[Li_{1/2}Fe_{1/2}Ti]O_4$ in non-aqueous lithium cells, Journal of Power Sources 146 (2005) 213.
[13] S.H. Huang, Z.Y. Wen, X.J. Zhu, Z.X. Lin, Effects of dopant on the electrochemical performance of $Li_4Ti_5O_{12}$ as electrode material for lithium ion batteries, Journal of Power Sources 165 (2007) 408.
[14] H.L. Zhao, Y. Li, Z.M. Zhu, J. Lin, Z.H. Tian, R.L. Wang, Structural and electrochemical characteristics of $Li_{4-x}Al_xTi_5O_{12}$ as anode material for lithium-ion batteries, Electrochimica Acta 53 (2008) 7079.
[15] G.J. Wang, J. Gao, L.J. Fu, N.H. Zhao, Y.P. Wu, T. Takamura, Preparation and characteristic of carbon-coated $Li_4Ti_5O_{12}$ anode material, Journal of Power Sources 174 (2007) 1109.
[16] J.-Y. Lin, C.-C. Hsu, H.-P. Ho, S.-H. Wu, Sol–gel synthesis of aluminum doped lithium titanate anode material for lithium ion batteries, Electrochimica Acta 87 (2010) 126.
[17] S.H. Huang, Z.Y. Wen, X.J. Zhu, Z.H. Gu, Preparation and electrochemical performance of Ag doped $Li_4Ti_5O_{12}$, Electrochemistry Communications 6 (2004) 1093.
[18] S.H. Huang, Z.Y. Wen, B. Lin, J.D. Han, X.G. Xu, The high-rate performance of the newly designed $Li_4Ti_5O_{12}$/Cu composite anode for lithium ion batteries, Journal of Alloys and Compounds 457 (2008) 400.
[19] R. Cai, X. Yu, X.Q. Liu, Z.P. Shao, $Li_4Ti_5O_{12}$/Sn composite anodes for lithium-ion batteries: synthesis and electrochemical performance, Journal of Power Sources 195 (2010) 8244.
[20] X. Li, M.Z. Qu, Y.J. Huai, Z.L. Yu, Preparation and electrochemical performance of $Li_4Ti_5O_{12}$/carbon/carbon nanotubes for lithium ion battery, Electrochimica Acta 55 (2010) 2978.
[21] H. Li, L.F. Shen, X.G. Zhang, J. Wang, P. Nie, Q. Che, B. Ding, Nitrogen-doped carbon coated $Li_4Ti_5O_{12}$ nanocomposite: superior anode materials for rechargeable lithium ion batteries, Journal of Power Sources 221 (2013) 122.
[22] D. Chen, L.H. Tang, J.H. Li, Graphene-based materials in electrochemistry, Chemical Society Reviews 39 (2010) 3157.
[23] P.C. Lian, X.F. Zhu, S.Z. Liang, Z. Li, W.S. Yang, H.H. Wang, High reversible capacity of SnO_2/graphene nanocomposite as an anode material for lithium-ion batteries, Electrochimica Acta 56 (2011) 4532.
[24] N. Zhu, W. Liu, M.Q. Xue, Z.A. Xie, D. Zhao, M.N. Zhang, J.T. Chen, T.B. Cao, Graphene as a conductive additive to enhance the high-rate capabilities of electrospun $Li_4Ti_5O_{12}$ for lithium-ion batteries, Electrochimica Acta 55 (2010) 5813.
[25] L.F. Shen, C.Z. Yuan, H.J. Luo, X.G. Zhang, S.D. Yang, X.J. Lu, In situ synthesis of high-loading $Li_4Ti_5O_{12}$–graphene hybrid nanostructures for high rate lithium ion batteries, Nanoscale 3 (2011) 572.
[26] Y.F. Tang, F.Q. Huang, W. Zhao, Z.Q. Liu, D.Y. Wan, Synthesis of graphene-supported $Li_4Ti_5O_{12}$ nanosheets for high rate battery application, Journal of Materials Chemistry 22 (2012) 11257.
[27] H.F. Xiang, B.B. Tian, P.C. Lian, Z. Li, H.H. Wang, Sol–gel synthesis and electrochemical performance of $Li_4Ti_5O_{12}$/graphene composite anode for lithium-ion batteries, Journal of Alloys and Compounds 509 (2011) 7205.
[28] Q. Zhang, W. Peng, Z. Wang, X. Li, X. Xiong, H. Guo, Z. Wang, F. Wu, $Li_4Ti_5O_{12}$/reduced graphene oxide composite as a high rate capability material for lithium ion batteries, Solid State Ionics 236 (2013) 30.
[29] Y. Ding, G.R. Li, C.W. Xiao, X.P. Gao, Insight into effects of graphene in $Li_4Ti_5O_{12}$/carbon composite with high rate capability as anode materials for lithium ion batteries, Electrochimica Acta 102 (2013) 282.
[30] P.C. Lian, X.F. Zhu, S.Z. Liang, Z. Li, W.S. Yang, H.H. Wang, Large reversible capacity of high quality graphene sheets as an anode material for lithium-ion batteries, Electrochimica Acta 55 (2010) 3909.
[31] G.N. Zhu, H.J. Liu, J.H. Zhuang, C.X. Wang, Y.G. Wang, Y.Y. Xia, Carbon-coated nano-sized $Li_4Ti_5O_{12}$ nanoporous micro-sphere as anode material for high-rate lithium-ion batteries, Energy and Environmental Science 4 (2011) 4016.
[32] X.F. Guo, C.Y. Wang, M.M. Chen, J.Z. Wang, J.M. Zheng, Carbon coating of $Li_4Ti_5O_{12}$ using amphiphilic carbonaceous material for improvement of lithium-ion battery performance, Journal of Power Sources 214 (2012) 107.
[33] H.F. Xiang, Q.Y. Jin, C.H. Chen, X.W. Ge, S. Guo, J.H. Sun, Dimethyl methylphosphonate-based nonflammable electrolyte and high safety lithium-ion batteries, Journal of Power Sources 174 (2007) 335.